2.5 Elasticity of cellular filaments

The bending deformation energy of a filament can be characterized by its flexural rigidity κ_f. Having units of [*energy* • *length*], the flexural rigidity of uniform rods can be written as a product of the Young's modulus Y (units of [*energy* • *length*^{3}]) and the moment of inertia of the cross section $\mathcal{I}$ (units of [*length*^{4}]): $\kappa_f = Y\mathcal{I}$. At finite temperature T, the rod's shape fluctuates, with the local orientation of the rod changing strongly over length scales characterized by the persistence length $\xi_p = \kappa_f / k_B T$, where k_B is Boltzmann's constant. We now review the experimental measurements of κ_f or ξ_p for a number of filaments in the cell, and then interpret them using results from Secs. 2.2 - 2.4.

Measurements of persistence length

Mechanical properties of the principal structural filaments of the cytoskeleton - spectrin, actin, intermediate filaments and microtubules - have been obtained through a variety of methods. In first determining the persistence length of spectrin, Stokke *et al*. (1985a) related the intrinsic viscosity of a spectrin dimer to its root-mean-square radius, from which the persistence length could be extracted via a relationship like Eq. (2.30). The resulting values of ξ_p covered a range of 15-25 nm, depending upon temperature. A more recent measurement (Svoboda *et al*., 1992) employs optical tweezers to hold a complete erythrocyte cytoskeleton in a flow chamber while the appearance of the cytoskeleton is observed as a function of the salt concentration of the medium. It is found that a persistence length of 10 nm is consistent with the mean squared end-to-end displacement $\langle r_{ee}^2 \rangle$ of the spectrin tetramer and with the dependence of the skeleton's diameter on salt concentration. Both measurements comfortably exceed the lower bound of 2.5 nm placed on the persistence length of a spectrin *monomer* by viewing it as a freely jointed chain of segment length b = 5 nm and invoking $\xi_p = b/2$ from Eqs. (2.31) and (2.35) [5 nm is the approximate length of each of approximately 20 barrel-like subunits in a spectrin monomer of contour length 100 nm; see Fig. 2.1(a)].

The persistence length of F-actin has been extracted from the analysis of perhaps a dozen experiments, although we cite here only a few recent works as an introduction to the literature. The measurements involve both native and fluorescently labelled actin filaments, which may account for some of the variation in the reported values of ξ_p. The principal techniques include:
(i) dynamic light scattering, which has given a rather broad range of results, the most recent converging on $\xi_p \sim 16$ μm (Janmey *et al*., 1994),
(ii) direct microscopic observation of the thermal fluctuations of fluorescently labelled actin filaments, as illustrated in Fig. 2.19. Actin filaments stabilized by phalloidin are observed to have $\xi_p = 18 \pm 1$ μm (Gittes *et al*., 1993; Isambert *et al*., 1995), while unstabilized actin filaments are more flexible, at $\xi_p = 9 \pm 0.5$ μm (Isambert *et al*., 1995),
(iii) direct microscopic observation of the driven oscillation of labelled actin filaments, giving $\xi_p = 7.4 \pm 0.2$ μm (Riveline *et al*., 1997).

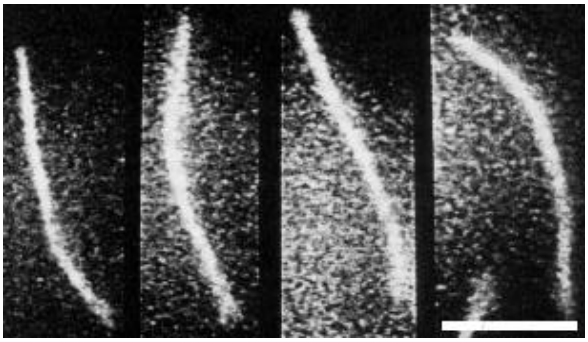

Fig. 2.19. Thermal fluctuations of a rhodamine-labelled actin filament observed by fluorescence microscopy at 6 second intervals. The bar is 5 mm in length (from Isambert *et al*., 1995).

Taken together, these experiments and others indicate that the persistence length of F-actin lies in the 10 - 20 μm range, about a thousand times larger than spectrin dimers.

Microtubules have been measured with several of the same techniques as employed for extracting the persistence length of actin filaments. Again, both pure and treated (in this case, taxol-stabilized) microtubules have been examined by means of:
(i) direct microscopic observation of the bending of microtubules as they move within a fluid medium, yielding ξ_p in the range of 1 - 8 mm (Venier *et al*., 1994; Kurz and Williams, 1995; Felgner *et al*., 1996),
(ii) direct microscopic observation of the thermal fluctuations of microtubules, giving a range of 1 - 6 mm (Gittes *et al*., 1993; Venier *et al*., 1994; Kurz and Williams, 1995),
(iii) direct microscopic observation of the buckling of a single, long microtubule confined within a vesicle under controlled conditions, leading to ξ_p = 6.3 mm (Elbaum *et al*., 1996).
Thus, the persistence length of microtubules is more than an order of magnitude larger than a typical cell diameter, with several measurements yielding results near the high end of the 1 - 6 mm range.

The filaments of the cytoskeleton are not the only polymers whose mechanical properties are important to the operation of the cell. For example, the packing of DNA into the restricted volume of the cell is a significant challenge, given both the contour length and persistence length of a DNA molecule. Measurements of the DNA persistence length date back at least a decade to the work of Taylor and Hagerman (1990), who found $\xi_p = 45 \pm 1.5$ nm by observing the rate at which a linear strand of DNA closes into a circle. A more recent experiment directly manipulates a single DNA molecule by attaching a magnetic bead to one end of the filament (while the other is held fixed) and applying a force by means of an external magnetic field. The resulting force-extension relation for DNA from bacteriophage lambda (a virus that attacks bacteria such as *E*. *coli*) is found to be well-described by the worm-like chain model, Eq. (2.66), which involves only two parameters - the contour length and the persistence length (Bustamante *et al*., 1994). As well as yielding a fitted contour length in agreement with the crystallographic value, the procedure gives a fitted

persistence length of 53 ± 2 nm, in the same range as found earlier by Taylor and Hagerman. Yet another approach records the motion of a fluorescently-labelled DNA molecule in a fluid (Perkins *et al*., 1995), the analysis of which gives $\xi_p \sim 68$ nm (Stigter and Bustamante, 1998), a slightly higher value than that of unlabelled DNA. The torsion resistance of DNA has also been measured (Strick *et al*., 1996).

The above measurements are summarized in Table 2.2, which also displays the mass per unit length of the filament (from Sec. 2.1). For comparison, the table includes alkanes with a very short persistence length (from Flory, 1969) and the tobacco mosaic virus, a hollow rod-like structure with a linear density similar to that of a microtubule and a persistence length to match. Experimentally, the flexural rigidity of the virus on a substrate is obtained by observing the response of the virus when probed by the tip of an atomic force microscope (Flavo *et al*., 1997). In this case and several others, the persistence length quoted in Table 2.2 is found from the flexural rigidity *via* Eq. (2.19).

ξ_p *and Young's modulus*

The measured persistence lengths in Table 2.2 span more than six orders of magnitude, a much larger range than the linear density, which covers about three orders of magnitude. We can understand this behavior by viewing the polymers as flexible rods, whose flexural rigidity from Eq. (2.9) is

$$\kappa_f = Y\mathcal{I}, \tag{2.67}$$

and corresponding persistence length, according to Eq. (2.19), is

$$\xi_p = Y\mathcal{I} / k_B T, \tag{2.68}$$

where the moment of inertia of the cross section for hollow rods of inner radius R_i and

Table 2.2. Linear density λ_p (mass per unit length) and persistence length ξ_p of some biologically important polymers.

Polymer	*Configuration*	λ_p (D/nm)	ξ_p (nm)
Long alkanes	linear polymer	~110	~0.5
Spectrin	2-strand filament	4,500	10-20
DNA	double helix	1,900	53 ± 2
F-actin	filament	16,000	10-20 x 10^3
Intermediate filaments	32 strand filament	~35,000	
Tobacco mosaic virus		~140,000	~1 x 10^6
Microtubules	13 protofilaments	160,000	1-6 x 10^6

outer radius R is [from Eq. (2.12)]

$$\mathcal{I} = \pi(R^4 - R_i^4)/4.$$

For some hollow biofilaments like the tobacco mosaic virus, for which $R/R_i \sim 4.5$, only a small error is introduced by neglecting R_i^4 in the expression for $\mathcal{I}$, so that

$$\xi_p \quad \pi Y R^4 / 4k_B T, \tag{2.69}$$

although we note that this expression is in error by a factor of two for microtubules ($R \sim$ 14 nm and $R_i \sim$ 11.5 nm; see Amos and Amos, 1991). Being raised to the fourth power, R must be known relatively well to make an accurate prediction with Eq. (2.69). Such is not always the case, and a somewhat gentler approach which, in some sense averages over the bumpy atomic boundary of a molecule, replaces R^2 by the mass per unit length λ_p using the relationship $\lambda_p = \rho_m \pi R^2$ for a cylinder, where ρ_m is the mass per unit volume. Thus, we obtain

$$\xi_p \quad (Y / 4\pi k_B T \rho_m^2)\, \lambda_p^2, \tag{2.70}$$

which implies that the persistence length should be proportional to the square of the mass per unit length, if Y and ρ_m are relatively constant from one filament to the next.

Data from Table 2.2 are plotted logarithmically in Fig. 2.20 as a test of the quadratic dependence of ξ_p on λ_p suggested by Eq. (2.70). With the exception of spectrin, which is a loosely intertwined pair of filaments, the data are consistent with

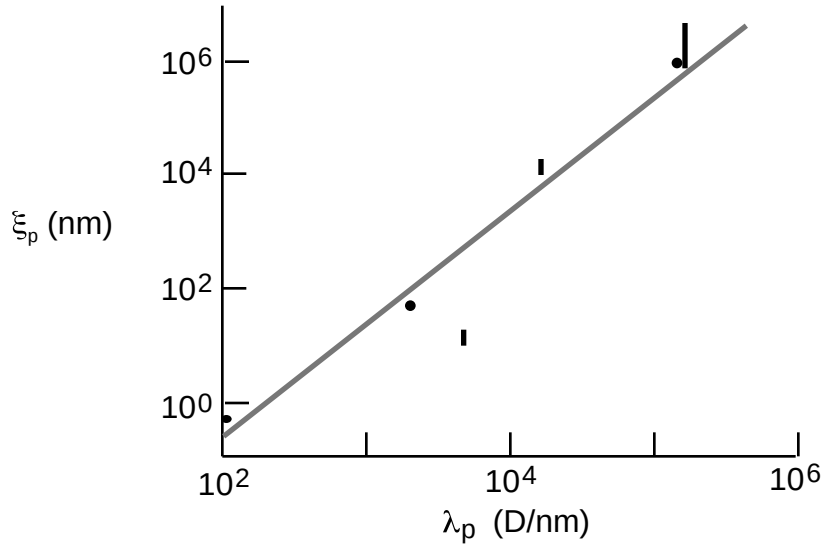

Fig. 2.20. Logarithmic plot of persistence length ξ_p against linear density λ_p for the data in Table 2.2. The straight line through the data is the function $\xi_p = 2.5 \times 10^{-5}\, \lambda_p^2$, where ξ_p is in nm and λ_p is in D/nm.

the fitted functional form $\xi_p = 2.5 \times 10^{-5} \lambda_p^2$, where ξ_p is in nm and λ_p is in D/nm. Because the data span so many orders of magnitude, the approximations (such as constant Y and ρ_m) behind the scaling law are supportable, and the graph can be used to find the Young's modulus of a generic biofilament. Equating the fitted numerical factor 2.5 x 10^{-5} nm^3/D^2 with $Y / 4\pi k_B T \rho_m^2$ gives $Y = 0.5 \times 10^9$ J/m^3 for $k_B T = 4 \times 10^{-21}$ J and $\rho_m = 10^3$ kg/m^3 (which is the density of water, or roughly the density of many hydrocarbons). Although no more accurate than a factor of two, this value of Y is in the same range as Y = 1-2 x 10^9 J/m^3 found for collagen (linear density of 1000 D/nm), but much smaller than that of dry cellulose (8 x 10^{10} J/m^3) or steel (2 x 10^{11} J/m^3). Of course, Eq. (2.70) can be applied to individual filaments if their radii and persistence lengths are sufficiently well-known, yielding $Y \sim (0.5 - 1.5) \times 10^9$ J/m^3 for most filaments.

Filament geometry and elasticity

How should the cytoskeletal filaments, whose flexural rigidities we now know, behave in the cell? As one representative situation, we examine microtubules, which can easily be as long as a typical cell is wide (say 10 μm) and have a persistence length one hundred times the cell diameter. Microtubules should not display very strong thermal oscillations, and indeed Eq. (2.18) demonstrates that the root mean square angle of oscillation $\langle\theta^2\rangle^{1/2}$ is about a tenth of a radian (or about 6 degrees) for a sample microtubule with L_c = 10 μm if the persistence length is in the mid-range of the experimental values, say $\xi_p = 2 \times 10^3$ μm. This doesn't mean that microtubules in the cell behave quite like steel rods in a plastic bag, as can be seen by the image in

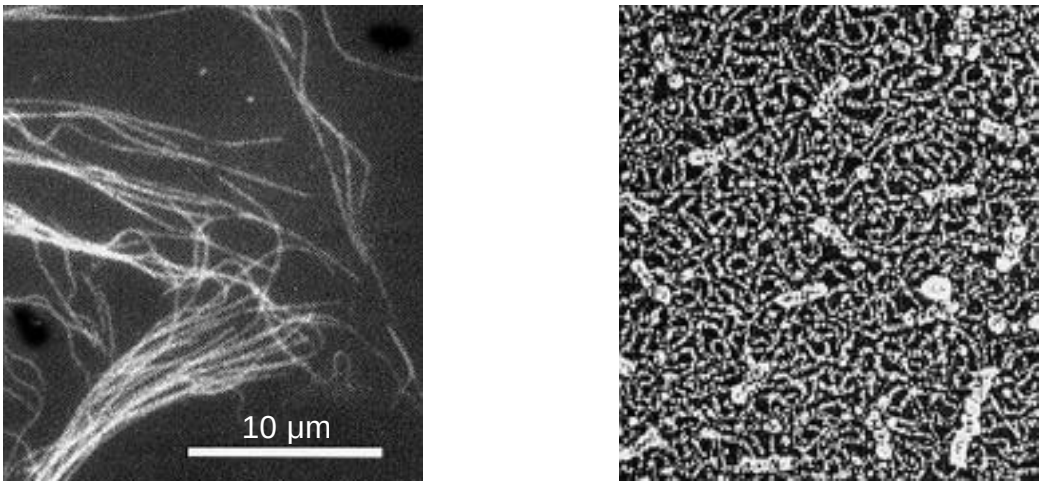

(a) (b)

Fig. 2.21. (a) Microtubules, with a persistence length in the millimeter range, are relatively stiff on cellular length scales (from Osborn, Webster and Weber, 1978), in contrast to spectrin (b), which has a persistence length five orders of magnitude smaller (spectrin network of the human erythrocyte, from Heuser, 1983).

Fig. 2.21(a), but a generous amount of energy is required to give our sample microtubule a substantial curvature: for example, $E_{arc} = (\xi_p / 2L_c)\, k_B T = 100\, k_B T$ if $R_c = L_c = 10$ μm, according to Eq. (2.14). Indeed, Elbaum *et al*. (1996) observe that a single microtubule with a length longer than the mean diameter of an artificial vesicle can cause the vesicle to deform into an ovoid.

Having a persistence length about one-tenth of its contour length, a spectrin tetramer should appear contorted on cellular length scales. In fact, its mean end-to-end displacement $\langle r_{ee}^2 \rangle^{1/2}$ is just 75 nm, which is only one-third of its contour length (200 nm), so the tetramers form a sinuous web when joined to form a network, as shown in Fig. 2.21(b). Thus, the network of spectrin tetramers in the human erythrocyte cytoskeleton can be stretched considerably to achieve a maximum area that is $(200/75)^2 \sim 7$ times its equilibrium area. As discussed in Sec. 2.4, highly convoluted chains such as spectrin resist extension, behaving like entropic springs with a spring constant $k_{sp} = 3k_B T / 2\xi_p L_c$ in three dimensions, from Eq. (2.62). Our spectrin tetramer, then, has a spring constant of about 2×10^{-6} J/m^2, which, although not a huge number, provides the cytoskeleton with enough shear resistance to restore a red cell to its equilibrium shape after passage through a narrow capillary. Lastly, we recall from the definition $\xi_p = \kappa_f / k_B T$ that the persistence length should decrease with temperature, if the flexural rigidity is temperature-independent. The temperature-dependence of the elasticity of biofilaments has not been as extensively studied as that of conventional polymers, but Stokke *et al*. (1985a) do find that the persistence length decreases with temperature roughly as expected for an entropic spring.

Summary

Sometimes criss-crossing the interior of a cell, sometimes forming a mat or wall around it, the biological chains and filaments of the cell range in diameter up to 25 nm and have a mass per unit length covering more than three orders of magnitude, from ~100 D/nm for alkanes to 160,000 D/nm for microtubules. A simple mathematical representation of these filaments views them as structureless lines characterized by a position $\mathbf{r}(s)$ and tangent vector $\mathbf{t}(s) = \partial\mathbf{r}(s)/\partial s$, where s is the arc length along the line. The lowest order expression for the energy per unit length of deforming a filament from its straight-line configuration is $(\kappa_f/2)(\partial\mathbf{t}(s)/\partial s)^2$, where κ_f is the flexural rigidity of the filament.

At non-zero temperature, filaments can exchange energy with their surroundings, permitting their shapes to fluctuate as they bend and twist. Their orientation changes direction with both position and time, such that the direction of the tangent vectors to the filament decays as $\langle \mathbf{t}(0) \bullet \mathbf{t}(s) \rangle = \exp(-s/\xi_p)$ due to thermal motion, where the persistence length $\xi_p = \kappa_f / k_B T$ depends upon the temperature T, k_B being Boltzmann's constant. Also, because of fluctuations, the squared end-to-end displacement $\mathbf{r}_{ee}$ of a filament is less than its contour length L_c, having the form $\langle r_{ee}^2 \rangle = 2\xi_p L_c - 2\xi_p^2 [1 - \exp(-L_c/\xi_p)]$, which approaches the rigid rod limit $\langle r_{ee}^2 \rangle^{1/2} \sim L_c$ only when $\xi_p >> L_c$. In comparison, long filaments with relatively short persistence lengths obey

form $\langle r_{ee}^2 \rangle = 2\xi_p L_c$, showing that the linear size of sinuous filaments grows only like the square root of the contour length, a property of all linear chains in which self-avoidance is neglected. When self-avoidance is enforced, the growth of $\langle r_{ee}^2 \rangle^{1/2}$ with L_c is dimension-dependent, achieving ideal behavior only in four dimensions. Branched polymers or linear chains with attractive interactions display still different scaling behavior.

At finite temperature, $\mathbf{r}_{ee}$ does not have a unique value but rather is distributed according to a probability per unit length of the form $\wp(x) = (2\pi\sigma^2)^{-1/2} \exp(-x^2 / 2\sigma^2)$ for filaments in one dimension, where x is the displacement from one end of the chain to the other. For freely jointed chains with N identical segments of length b, the variance $\sigma^2 = Nb^2/d$, where d is the spatial dimension of the chain. This distribution, and its three-dimensional cousin, demonstrate that a chain is not likely to be found in its fully stretched configuration $r_{ee} = L_c$ because such a configuration is strongly disfavored by entropy. Thus, the free energy of a flexible chain rises as the chain is stretched from its equilibrium value of r_{ee}, and the chain behaves like an entropic spring with a force constant $k_{sp} = 3k_B T / 2\xi_p L_c = 3k_B T / \langle r_{ee}^2 \rangle$ in three dimensions.

The persistence lengths of a variety of the cell's polymers and filaments have been measured, and they span the enormous range of 0.5 nm for alkanes up to a few millimeters for microtubules. This behavior can be understood by viewing the filament as a flexible rod of uniform density and cross section, permitting the flexural rigidity to be written as $\kappa_f = Y\mathcal{I}$, where Y is the material's Young's modulus. The moment of inertia of the cross section $\mathcal{I}$ has the form $\mathcal{I} = \pi(R^4 - R_i^4)/4$ for a hollow tube of inner and outer radii R_i and R, respectively, predicting that the persistence length has the form $\xi_p = \pi Y(R^4 - R_i^4) / 4k_B T$. Treated as uniform rods, the filaments of the cell have Young's moduli in the range $(0.5 - 1.5) \times 10^9$ J/m^3, which is about two orders of magnitude lower than the moduli of conventionally "hard" materials such as wood or steel, but comparable to plastics.

Problems

Biological applications

2.1. Consider a large motor neuron running from the brain to the arm containing a core bundle of microtubules. Taking the persistence length of a microtubule to be 2 mm, what energy is required (in $k_B T$ at 300 K) to bend a 20 cm long microtubule into an arc of radius 10 cm?

2.2. Let θ be the angle characterizing the change in direction of a filament along its length. For a tobacco mosaic virus of contour length 250 nm, determine the value of $\langle \theta^2 \rangle^{1/2}$ arising from thermal fluctuations. Quote your answer in degrees.

2.3. Consider a piece of spaghetti 2 mm in diameter. If the Young's modulus Y of this material is 1×10^8 J/m^3, what is its persistence length at $T = 300$ K? Is the result consistent with your everyday observations?

2.4. Flagella are whip-like structures typically about 10 μm long whose bending resistance arises from a microtubule core. Treating the flagellum as a hollow rod of inner radius 0.07 μm and outer radius 0.1 μm, find its persistence length at T = 300 K if its Young's modulus is 1 x 10^8 J/m^3. Compare your result with the persistence length of a single microtubule. (*Note: this approximation is not especially trustworthy)*

2.5. What are the structural advantages for a microtubule to be hollow? Calculate the mass ratio and the flexural rigidity ratio for a hollow microtubule with inner and outer radii 11.5 and 14 nm, respectively, compared to a solid microtubule with the same outer radius. What is the most efficient use of proteins to gain rigidity: one solid microtubule or several hollow ones?

2.6. The virus bacteriophage-λ contains a string of 97000 base pairs in its DNA. Find the length of this DNA strand at 0.34 nm/base-pair and compare it to the DNA persistence length. If the DNA is 2 nm in diameter, what is the radius of the smallest spherical volume into which it can be packed? If this DNA becomes a random chain once released into a host cell, what is its root mean square end-to-end distance? Compare your answers to the size of a typical bacterium.

2.7. Compare root mean square end-to-end distance $\langle r_{ee}^2 \rangle^{1/2}$ of strands of spectrin, actin and microtubules 200 nm in contour length. What is the effective spring constant for each protein, for filaments with a contour length of 1 cm at 300 K? Use ξ_p = 15, 15 x 10^3, and 2 x 10^6 nm for spectrin, actin and microtubules, respectively.

2.8. Consider a 30 μm length of DNA, such as might be found in a virus. What force is required to stretch the DNA to an end-to-end displacement x = 10, 20 and 25 μm, according to the Gaussian approximation Eq. (2.62) and the worm-like chain model Eq. (2.66)? Assume the temperature is 300 K.

Formal development and extensions

2.9. Consider a polymer such as a linear alkane, where the bond angle between successive carbon atoms is a fixed value α, although the bonds are free to rotate around one another.

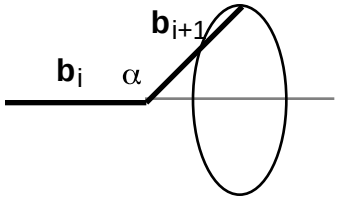

The length and orientation of the bond between atom i and atom i+1 defines a bond vector $\mathbf{b}_i$. Assume all bond lengths are the same, and that remote bonds can intersect.
(a) Show that the average projection of $\mathbf{b}_{i+k}$ on $\mathbf{b}_i$ is

$$\langle \mathbf{b}_i \bullet \mathbf{b}_{i+k} \rangle = b^2(-\cos\alpha)^k \qquad (k \geq 0)$$

[*Hint: start with* $\langle \mathbf{b}_i \bullet \mathbf{b}_{i+1} \rangle$ *and iterate*]
(b) Write $\langle \mathbf{r}_{ee}^2 \rangle$ in terms of $\langle \mathbf{b}_i \bullet \mathbf{b}_j \rangle$ to obtain

$$\langle \mathbf{r}_{ee}^2 \rangle / b^2 = N\,[1 + (2 - 2/N)(-\cos\alpha) + (2 - 4/N)(-\cos\alpha)^2 + ...].$$

(c) Use your result from (b) to establish that, in the large N limit

$$\langle \mathbf{r}_{ee}^2 \rangle = Nb^2 (1 - \cos\alpha) / (1 + \cos\alpha)$$

(d) What is the effective bond length (in units of b) in this model at the tetrahedral value of 109.5°?

2.10. The backbone of polymers such as the polysiloxanes have alternating unequal bond angles:

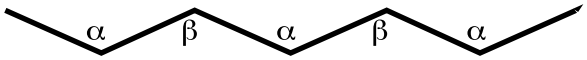

even though the bond lengths are all equal.

(a) Show that, if self-intersections of this type of chain are permitted, its effective bond length is $B_{eff}^2 = b^2 (1 - \cos\alpha)\bullet(1 - \cos\beta) / (1 - \cos\alpha \cos\beta)$. [*Hint: follow the same steps as in Prob. 2.9*]

(b) Confirm that this expression reduces to the fixed-angle rotating chain expression in Prob. 2.9(c) when $\alpha = \beta$.

(c) Evaluate B_{eff} when $\alpha = 109.5°$, $\beta = 130°$ and $b = 0.17$ nm.

2.11. Show that $\langle|\mathbf{r}_{ee}|\rangle = (8/3\pi)^{1/2} N^{1/2} b$ for ideal chains in three dimensions.

2.12. The radius of gyration, or root mean square radius, R_g of the N+1 vertices in a linear chain, is defined by

$$R_g^2 = [\Sigma_{i=1,N+1} (\mathbf{r}_i - \mathbf{r}_{cm})^2] / (N+1)$$

where $\mathbf{r}_i$ is the position vector of each of the N+1 vertices and $\mathbf{r}_{cm}$ is the center-of-mass position $\mathbf{r}_{cm} = \Sigma_i \mathbf{r}_i / (N+1)$. Show that $\langle R_g^2 \rangle = \langle r_{ee}^2 \rangle / 6$ for ideal chains.

[*Hint: recast the problem to read* $R_g^2 \quad \Sigma\Sigma\, r_{ij}^2$ *and then use* $\langle r_{ij}^2 \rangle = |j - i| b^2$ *where* $\mathbf{r}_{ij}$ *is the displacement between vertices* i *and* j. *Justify!*]

2.13. Find $r_{ee,\ most\ likely}$ and $\langle|\mathbf{r}_{ee}|\rangle$ for ideal chains in two dimensions.

2.14. Suppose that a particle moves only in one direction at a constant speed v but changes direction randomly at the end of every time interval Δt.

(a) Find the diffusion constant D of the motion as a function of v and Δt, given the diffusion equation $\langle x^2 \rangle = 2Dt$.

(b) Find the temperature dependence of D if the kinetic energy of the particle is $k_B T/2$.

2.15. Consider a three-dimensional ideal chain of 50 segments, each with length 10 nm.

(a) What is $\langle|\mathbf{r}_{ee}|\rangle$ and $\langle \mathbf{r}_{ee}^2 \rangle^{1/2}$?

(b) What is the effective spring constant at 300 K?

(c) If the chain has charges +/-e on each end and is placed in a field of 10^6 V/m, what is the change in the end-to-end distance?

2.16. The results in the text for the distribution of $\mathbf{r}_{ee}$ for random chains in three dimensions can be generalized easily to random chains in d dimensions. For chains whose N segments have a uniform length b, show that:

(a) the distribution of end-to-end distances has the conventional Gaussian form, but with $\sigma^2 = Nb^2/d$.
(b) the effective spring constant is $k_{sp} = dk_B T / Nb^2$.

2.17. Compare the flexural rigidity of the solid cylindrical rod of Eq. (2.11) with a solid rod with the cross section of a square. Take both rods to have the same cross sectional area πR^2. Place the axis of symmetry through the center of the square.

2.18. Determine the moment of inertia of the cross section for the three regular-shaped rods with cross sections:

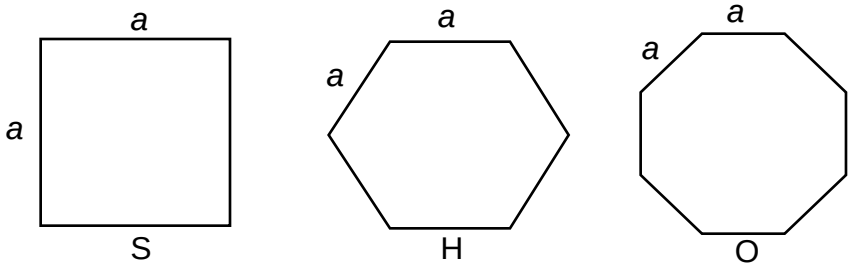

Take the length of the side in each case to be a. Find the ratio of these moments to that of a cylinder of radius R ($\mathcal{I} = \pi R^4/4$), imposing the condition that all shapes have the same cross sectional area πR^2 to express a in terms of R.

2.19. Compare the two force-extension relations in Eqs. (2.64) and (2.66) by plotting ($2\xi_p f/k_B T$) against x/L_c. At what value of x/L_c is the difference between these curves the largest?